

Search for Standard Model Higgs Bosons Produced in Association with W Bosons

T. Aaltonen,²³ J. Adelman,¹³ T. Akimoto,⁵⁴ M.G. Albrow,¹⁷ B. Álvarez González,¹¹
 S. Amerio,⁴² D. Amidei,³⁴ A. Anastassov,⁵¹ A. Annovi,¹⁹ J. Antos,¹⁴ M. Aoki,²⁴
 G. Apollinari,¹⁷ A. Apresyan,⁴⁷ T. Arisawa,⁵⁶ A. Artikov,¹⁵ W. Ashmanskas,¹⁷
 A. Attal,³ A. Aurisano,⁵² F. Azfar,⁴¹ P. Azzi-Bacchetta,⁴² P. Azzurri,⁴⁵ N. Bacchetta,⁴²
 W. Badgett,¹⁷ A. Barbaro-Galtieri,²⁸ V.E. Barnes,⁴⁷ B.A. Barnett,²⁵ S. Baroiant,⁷
 V. Bartsch,³⁰ G. Bauer,³² P.-H. Beauchemin,³³ F. Bedeschi,⁴⁵ P. Bednar,¹⁴
 S. Behari,²⁵ G. Bellettini,⁴⁵ J. Bellinger,⁵⁸ A. Belloni,²² D. Benjamin,¹⁶ A. Beretvas,¹⁷
 J. Beringer,²⁸ T. Berry,²⁹ A. Bhatti,⁴⁹ M. Binkley,¹⁷ D. Bisello,⁴² I. Bizjak,³⁰
 R.E. Blair,² C. Blocker,⁶ B. Blumenfeld,²⁵ A. Bocci,¹⁶ A. Bodek,⁴⁸ V. Boisvert,⁴⁸
 G. Bolla,⁴⁷ A. Bolshov,³² D. Bortoletto,⁴⁷ J. Boudreau,⁴⁶ A. Boveia,¹⁰ B. Brau,¹⁰
 A. Bridgeman,²⁴ L. Brigliadori,⁵ C. Bromberg,³⁵ E. Brubaker,¹³ J. Budagov,¹⁵
 H.S. Budd,⁴⁸ S. Budd,²⁴ K. Burkett,¹⁷ G. Busetto,⁴² P. Bussey,²¹ A. Buzatu,³³
 K. L. Byrum,² S. Cabrera^r,¹⁶ M. Campanelli,³⁵ M. Campbell,³⁴ F. Canelli,¹⁷ A. Canepa,⁴⁴
 D. Carlsmith,⁵⁸ R. Carosi,⁴⁵ S. Carrillo^l,¹⁸ S. Carron,³³ B. Casal,¹¹ M. Casarsa,¹⁷
 A. Castro,⁵ P. Catastini,⁴⁵ D. Cauz,⁵³ M. Cavalli-Sforza,³ A. Cerri,²⁸ L. Cerrito^p,³⁰
 S.H. Chang,²⁷ Y.C. Chen,¹ M. Chertok,⁷ G. Chiarelli,⁴⁵ G. Chlachidze,¹⁷ F. Chlebana,¹⁷
 K. Cho,²⁷ D. Chokheli,¹⁵ J.P. Chou,²² G. Choudalakis,³² S.H. Chuang,⁵¹ K. Chung,¹²
 W.H. Chung,⁵⁸ Y.S. Chung,⁴⁸ C.I. Ciobanu,²⁴ M.A. Ciocci,⁴⁵ A. Clark,²⁰ D. Clark,⁶
 G. Compostella,⁴² M.E. Convery,¹⁷ J. Conway,⁷ B. Cooper,³⁰ K. Copic,³⁴ M. Cordelli,¹⁹
 G. Cortiana,⁴² F. Crescioli,⁴⁵ C. Cuenca Almenar^r,⁷ J. Cuevas^o,¹¹ R. Culbertson,¹⁷
 J.C. Cully,³⁴ D. Dagenhart,¹⁷ M. Datta,¹⁷ T. Davies,²¹ P. de Barbaro,⁴⁸ S. De Cecco,⁵⁰
 A. Deisher,²⁸ G. De Lentdecker^d,⁴⁸ G. De Lorenzo,³ M. Dell'Orso,⁴⁵ L. Demortier,⁴⁹
 J. Deng,¹⁶ M. Deninno,⁵ D. De Pedis,⁵⁰ P.F. Derwent,¹⁷ G.P. Di Giovanni,⁴³ C. Dionisi,⁵⁰
 B. Di Ruzza,⁵³ J.R. Dittmann,⁴ M. D'Onofrio,³ S. Donati,⁴⁵ P. Dong,⁸ J. Donini,⁴²
 T. Dorigo,⁴² S. Dube,⁵¹ J. Efron,³⁸ R. Erbacher,⁷ D. Errede,²⁴ S. Errede,²⁴ R. Eusebi,¹⁷
 H.C. Fang,²⁸ S. Farrington,²⁹ W.T. Fedorko,¹³ R.G. Feild,⁵⁹ M. Feindt,²⁶ J.P. Fernandez,³¹
 C. Ferrazza,⁴⁵ R. Field,¹⁸ G. Flanagan,⁴⁷ R. Forrest,⁷ S. Forrester,⁷ M. Franklin,²²
 J.C. Freeman,²⁸ I. Furic,¹⁸ M. Gallinaro,⁴⁹ J. Galyardt,¹² F. Garbersen,¹⁰ J.E. Garcia,⁴⁵

A.F. Garfinkel,⁴⁷ H. Gerberich,²⁴ D. Gerdes,³⁴ S. Giagu,⁵⁰ V. Giakoumopolou^{a, 45}
 P. Giannetti,⁴⁵ K. Gibson,⁴⁶ J.L. Gimmell,⁴⁸ C.M. Ginsburg,¹⁷ N. Giokaris^{a, 15}
 M. Giordani,⁵³ P. Giromini,¹⁹ M. Giunta,⁴⁵ V. Glagolev,¹⁵ D. Glenzinski,¹⁷ M. Gold,³⁶
 N. Goldschmidt,¹⁸ A. Golossanov,¹⁷ G. Gomez,¹¹ G. Gomez-Ceballos,³² M. Goncharov,⁵²
 O. González,³¹ I. Gorelov,³⁶ A.T. Goshaw,¹⁶ K. Goulianos,⁴⁹ A. Gresele,⁴² S. Grinstein,²²
 C. Grosso-Pilcher,¹³ R.C. Group,¹⁷ U. Grundler,²⁴ J. Guimaraes da Costa,²²
 Z. Gunay-Unalan,³⁵ C. Haber,²⁸ K. Hahn,³² S.R. Hahn,¹⁷ E. Halkiadakis,⁵¹ A. Hamilton,²⁰
 B.-Y. Han,⁴⁸ J.Y. Han,⁴⁸ R. Handler,⁵⁸ F. Happacher,¹⁹ K. Hara,⁵⁴ D. Hare,⁵¹ M. Hare,⁵⁵
 S. Harper,⁴¹ R.F. Harr,⁵⁷ R.M. Harris,¹⁷ M. Hartz,⁴⁶ K. Hatakeyama,⁴⁹ J. Hauser,⁸
 C. Hays,⁴¹ M. Heck,²⁶ A. Heijboer,⁴⁴ B. Heinemann,²⁸ J. Heinrich,⁴⁴ C. Henderson,³²
 M. Herndon,⁵⁸ J. Heuser,²⁶ S. Hewamanage,⁴ D. Hidas,¹⁶ C.S. Hill^{c, 10} D. Hirschbuehl,²⁶
 A. Hocker,¹⁷ S. Hou,¹ M. Houlden,²⁹ S.-C. Hsu,⁹ B.T. Huffman,⁴¹ R.E. Hughes,³⁸
 U. Husemann,⁵⁹ J. Huston,³⁵ J. Incandela,¹⁰ G. Introzzi,⁴⁵ M. Iori,⁵⁰ A. Ivanov,⁷
 B. Iyutin,³² E. James,¹⁷ B. Jayatilaka,¹⁶ D. Jeans,⁵⁰ E.J. Jeon,²⁷ S. Jindariani,¹⁸
 W. Johnson,⁷ M. Jones,⁴⁷ K.K. Joo,²⁷ S.Y. Jun,¹² J.E. Jung,²⁷ T.R. Junk,²⁴ T. Kamon,⁵²
 D. Kar,¹⁸ P.E. Karchin,⁵⁷ Y. Kato,⁴⁰ R. Kephart,¹⁷ U. Kerzel,²⁶ V. Khotilovich,⁵²
 B. Kilminster,³⁸ D.H. Kim,²⁷ H.S. Kim,²⁷ J.E. Kim,²⁷ M.J. Kim,¹⁷ S.B. Kim,²⁷ S.H. Kim,⁵⁴
 Y.K. Kim,¹³ N. Kimura,⁵⁴ L. Kirsch,⁶ S. Klimenko,¹⁸ M. Klute,³² B. Knuteson,³² B.R. Ko,¹⁶
 S.A. Koay,¹⁰ K. Kondo,⁵⁶ D.J. Kong,²⁷ J. Konigsberg,¹⁸ A. Korytov,¹⁸ A.V. Kotwal,¹⁶
 J. Kraus,²⁴ M. Kreps,²⁶ J. Kroll,⁴⁴ N. Krumnack,⁴ M. Kruse,¹⁶ V. Krutelyov,¹⁰
 T. Kubo,⁵⁴ S. E. Kuhlmann,² T. Kuhr,²⁶ N.P. Kulkarni,⁵⁷ Y. Kusakabe,⁵⁶ S. Kwang,¹³
 A.T. Laasanen,⁴⁷ S. Lai,³³ S. Lami,⁴⁵ S. Lammel,¹⁷ M. Lancaster,³⁰ R.L. Lander,⁷
 K. Lannon,³⁸ A. Lath,⁵¹ G. Latino,⁴⁵ I. Lazzizzera,⁴² T. LeCompte,² J. Lee,⁴⁸ J. Lee,²⁷
 Y.J. Lee,²⁷ S.W. Lee^{q, 52} R. Lefèvre,²⁰ N. Leonardo,³² S. Leone,⁴⁵ S. Levy,¹³ J.D. Lewis,¹⁷
 C. Lin,⁵⁹ C.S. Lin,²⁸ J. Linacre,⁴¹ M. Lindgren,¹⁷ E. Lipeles,⁹ A. Lister,⁷ D.O. Litvintsev,¹⁷
 T. Liu,¹⁷ N.S. Lockyer,⁴⁴ A. Loginov,⁵⁹ M. Loreti,⁴² L. Lovas,¹⁴ R.-S. Lu,¹ D. Lucchesi,⁴²
 J. Lueck,²⁶ C. Luci,⁵⁰ P. Lujan,²⁸ P. Lukens,¹⁷ G. Lungu,¹⁸ L. Lyons,⁴¹ J. Lys,²⁸ R. Lysak,¹⁴
 E. Lytken,⁴⁷ P. Mack,²⁶ D. MacQueen,³³ R. Madrak,¹⁷ K. Maeshima,¹⁷ K. Makhoul,³²
 T. Maki,²³ P. Maksimovic,²⁵ S. Malde,⁴¹ S. Malik,³⁰ G. Manca,²⁹ A. Manousakis^{a, 15}
 F. Margaroli,⁴⁷ C. Marino,²⁶ C.P. Marino,²⁴ A. Martin,⁵⁹ M. Martin,²⁵ V. Martin^{j, 21}

M. Martínez,³ R. Martínez-Ballarín,³¹ T. Maruyama,⁵⁴ P. Mastrandrea,⁵⁰ T. Masubuchi,⁵⁴
M.E. Mattson,⁵⁷ P. Mazzanti,⁵ K.S. McFarland,⁴⁸ P. McIntyre,⁵² R. McNulty,²⁹
A. Mehta,²⁹ P. Mehtala,²³ S. Menzemer,^{k,11} A. Menzione,⁴⁵ P. Merkel,⁴⁷ C. Mesropian,⁴⁹
A. Messina,³⁵ T. Miao,¹⁷ N. Miladinovic,⁶ J. Miles,³² R. Miller,³⁵ C. Mills,²² M. Milnik,²⁶
A. Mitra,¹ G. Mitselmakher,¹⁸ H. Miyake,⁵⁴ S. Moed,²² N. Moggi,⁵ C.S. Moon,²⁷
R. Moore,¹⁷ M. Morello,⁴⁵ P. Movilla Fernandez,²⁸ J. Mülmenstädt,²⁸ A. Mukherjee,¹⁷
Th. Muller,²⁶ R. Mumford,²⁵ P. Murat,¹⁷ M. Mussini,⁵ J. Nachtman,¹⁷ Y. Nagai,⁵⁴
A. Nagano,⁵⁴ J. Naganoma,⁵⁶ K. Nakamura,⁵⁴ I. Nakano,³⁹ A. Napier,⁵⁵ V. Necula,¹⁶
C. Neu,⁴⁴ M.S. Neubauer,²⁴ J. Nielsen,^{f,28} L. Nodulman,² M. Norman,⁹ O. Norniella,²⁴
E. Nurse,³⁰ S.H. Oh,¹⁶ Y.D. Oh,²⁷ I. Oksuzian,¹⁸ T. Okusawa,⁴⁰ R. Oldeman,²⁹ R. Orava,²³
K. Osterberg,²³ S. Pagan Griso,⁴² C. Pagliarone,⁴⁵ E. Palencia,¹⁷ V. Papadimitriou,¹⁷
A. Papaikonomou,²⁶ A.A. Paramonov,¹³ B. Parks,³⁸ S. Pashapour,³³ J. Patrick,¹⁷
G. Pauletta,⁵³ M. Paulini,¹² C. Paus,³² D.E. Pellett,⁷ A. Penzo,⁵³ T.J. Phillips,¹⁶
G. Piacentino,⁴⁵ J. Piedra,⁴³ L. Pinera,¹⁸ K. Pitts,²⁴ C. Plager,⁸ L. Pondrom,⁵⁸ X. Portell,³
O. Poukhov,¹⁵ N. Pounder,⁴¹ F. Prakoshyn,¹⁵ A. Pronko,¹⁷ J. Proudfoot,² F. Ptohos,^{h,17}
G. Punzi,⁴⁵ J. Pursley,⁵⁸ J. Rademacker,^{c,41} A. Rahaman,⁴⁶ V. Ramakrishnan,⁵⁸
N. Ranjan,⁴⁷ I. Redondo,³¹ B. Reisert,¹⁷ V. Rekovic,³⁶ P. Renton,⁴¹ M. Rescigno,⁵⁰
S. Richter,²⁶ F. Rimondi,⁵ L. Ristori,⁴⁵ A. Robson,²¹ T. Rodrigo,¹¹ E. Rogers,²⁴ S. Rolli,⁵⁵
R. Roser,¹⁷ M. Rossi,⁵³ R. Rossin,¹⁰ P. Roy,³³ A. Ruiz,¹¹ J. Russ,¹² V. Rusu,¹⁷
H. Saarikko,²³ A. Safonov,⁵² W.K. Sakumoto,⁴⁸ G. Salamanna,⁵⁰ O. Saltó,³ L. Santi,⁵³
S. Sarkar,⁵⁰ L. Sartori,⁴⁵ K. Sato,¹⁷ A. Savoy-Navarro,⁴³ T. Scheidle,²⁶ P. Schlabach,¹⁷
E.E. Schmidt,¹⁷ M.A. Schmidt,¹³ M.P. Schmidt,⁵⁹ M. Schmitt,³⁷ T. Schwarz,⁷
L. Scodellaro,¹¹ A.L. Scott,¹⁰ A. Scribano,⁴⁵ F. Scuri,⁴⁵ A. Sedov,⁴⁷ S. Seidel,³⁶ Y. Seiya,⁵⁰
A. Semenov,¹⁵ L. Sexton-Kennedy,¹⁷ A. Sfyria,²⁰ S.Z. Shalhout,⁵⁷ M.D. Shapiro,²⁸
T. Shears,²⁹ P.F. Shepard,⁴⁶ D. Sherman,²² M. Shimojima,^{n,54} M. Shochet,¹³ Y. Shon,⁵⁸
I. Shreyber,²⁰ A. Sidoti,⁴⁵ J. Siegrist,²⁸ P. Sinervo,³³ A. Sisakyan,¹⁵ A.J. Slaughter,¹⁷
J. Slaunwhite,³⁸ K. Sliwa,⁵⁵ J.R. Smith,⁷ F.D. Snider,¹⁷ R. Snihur,³³ M. Soderberg,³⁴
A. Soha,⁷ S. Somalwar,⁵¹ V. Sorin,³⁵ J. Spalding,¹⁷ F. Spinella,⁴⁵ T. Spreitzer,³³
P. Squillacioti,⁴⁵ M. Stanitzki,⁵⁹ R. St. Denis,²¹ B. Stelzer,⁸ O. Stelzer-Chilton,⁴¹
D. Stentz,³⁷ J. Strogas,³⁶ D. Stuart,¹⁰ J.S. Suh,²⁷ A. Sukhanov,¹⁸ H. Sun,⁵⁵ I. Suslov,¹⁵

T. Suzuki,⁵⁴ A. Taffard^e,²⁴ R. Takashima,³⁹ Y. Takeuchi,⁵⁴ R. Tanaka,³⁹ M. Tecchio,³⁴ P.K. Teng,¹ K. Terashi,⁴⁹ J. Thom^g,¹⁷ A.S. Thompson,²¹ G.A. Thompson,²⁴ E. Thomson,⁴⁴ P. Tipton,⁵⁹ V. Tiwari,¹² S. Tkaczyk,¹⁷ D. Toback,⁵² S. Tokar,¹⁴ K. Tollefson,³⁵ T. Tomura,⁵⁴ D. Tonelli,¹⁷ S. Torre,¹⁹ D. Torretta,¹⁷ S. Tourneur,⁴³ W. Trischuk,³³ Y. Tu,⁴⁴ N. Turini,⁴⁵ F. Ukegawa,⁵⁴ S. Uozumi,⁵⁴ S. Vallecorsa,²⁰ N. van Remortel,²³ A. Varganov,³⁴ E. Vataga,³⁶ F. Vázquez^l,¹⁸ G. Velev,¹⁷ C. Vellidis^a,⁴⁵ V. Veszpremi,⁴⁷ M. Vidal,³¹ R. Vidal,¹⁷ I. Vila,¹¹ R. Vilar,¹¹ T. Vine,³⁰ M. Vogel,³⁶ I. Volobouev^q,²⁸ G. Volpi,⁴⁵ F. Würthwein,⁹ P. Wagner,⁴⁴ R.G. Wagner,² R.L. Wagner,¹⁷ J. Wagner-Kuhr,²⁶ W. Wagner,²⁶ T. Wakisaka,⁴⁰ R. Wallny,⁸ S.M. Wang,¹ A. Warburton,³³ D. Waters,³⁰ M. Weinberger,⁵² W.C. Wester III,¹⁷ B. Whitehouse,⁵⁵ D. Whiteson^e,⁴⁴ A.B. Wicklund,² E. Wicklund,¹⁷ G. Williams,³³ H.H. Williams,⁴⁴ P. Wilson,¹⁷ B.L. Winer,³⁸ P. Wittich^g,¹⁷ S. Wolbers,¹⁷ C. Wolfe,¹³ T. Wright,³⁴ X. Wu,²⁰ S.M. Wynne,²⁹ A. Yagil,⁹ K. Yamamoto,⁴⁰ J. Yamaoka,⁵¹ T. Yamashita,³⁹ C. Yang,⁵⁹ U.K. Yang^m,¹³ Y.C. Yang,²⁷ W.M. Yao,²⁸ G.P. Yeh,¹⁷ J. Yoh,¹⁷ K. Yorita,¹³ T. Yoshida,⁴⁰ G.B. Yu,⁴⁸ I. Yu,²⁷ S.S. Yu,¹⁷ J.C. Yun,¹⁷ L. Zanello,⁵⁰ A. Zanetti,⁵³ I. Zaw,²² X. Zhang,²⁴ Y. Zheng^b,⁸ and S. Zucchelli⁵

(CDF Collaboration*)

¹*Institute of Physics, Academia Sinica,
Taipei, Taiwan 11529, Republic of China*

²*Argonne National Laboratory, Argonne, Illinois 60439*

³*Institut de Fisica d'Altes Energies,
Universitat Autònoma de Barcelona,
E-08193, Bellaterra (Barcelona), Spain*

* With visitors from ^aUniversity of Athens, 15784 Athens, Greece, ^bChinese Academy of Sciences, Beijing 100864, China, ^cUniversity of Bristol, Bristol BS8 1TL, United Kingdom, ^dUniversity Libre de Bruxelles, B-1050 Brussels, Belgium, ^eUniversity of California Irvine, Irvine, CA 92697, ^fUniversity of California Santa Cruz, Santa Cruz, CA 95064, ^gCornell University, Ithaca, NY 14853, ^hUniversity of Cyprus, Nicosia CY-1678, Cyprus, ⁱUniversity College Dublin, Dublin 4, Ireland, ^jUniversity of Edinburgh, Edinburgh EH9 3JZ, United Kingdom, ^kUniversity of Heidelberg, D-69120 Heidelberg, Germany, ^lUniversidad Iberoamericana, Mexico D.F., Mexico, ^mUniversity of Manchester, Manchester M13 9PL, England, ⁿNagasaki Institute of Applied Science, Nagasaki, Japan, ^oUniversity de Oviedo, E-33007 Oviedo, Spain, ^pQueen Mary, University of London, London, E1 4NS, England, ^qTexas Tech University, Lubbock, TX 79409, ^rIFIC(CSIC-Universitat de Valencia), 46071 Valencia, Spain,

- ⁴*Baylor University, Waco, Texas 76798*
- ⁵*Istituto Nazionale di Fisica Nucleare,
University of Bologna, I-40127 Bologna, Italy*
- ⁶*Brandeis University, Waltham, Massachusetts 02254*
- ⁷*University of California, Davis, Davis, California 95616*
- ⁸*University of California, Los Angeles, Los Angeles, California 90024*
- ⁹*University of California, San Diego, La Jolla, California 92093*
- ¹⁰*University of California, Santa Barbara, Santa Barbara, California 93106*
- ¹¹*Instituto de Fisica de Cantabria, CSIC-University of Cantabria, 39005 Santander, Spain*
- ¹²*Carnegie Mellon University, Pittsburgh, PA 15213*
- ¹³*Enrico Fermi Institute, University of Chicago, Chicago, Illinois 60637*
- ¹⁴*Comenius University, 842 48 Bratislava,
Slovakia; Institute of Experimental Physics, 040 01 Kosice, Slovakia*
- ¹⁵*Joint Institute for Nuclear Research, RU-141980 Dubna, Russia*
- ¹⁶*Duke University, Durham, North Carolina 27708*
- ¹⁷*Fermi National Accelerator Laboratory, Batavia, Illinois 60510*
- ¹⁸*University of Florida, Gainesville, Florida 32611*
- ¹⁹*Laboratori Nazionali di Frascati, Istituto Nazionale
di Fisica Nucleare, I-00044 Frascati, Italy*
- ²⁰*University of Geneva, CH-1211 Geneva 4, Switzerland*
- ²¹*Glasgow University, Glasgow G12 8QQ, United Kingdom*
- ²²*Harvard University, Cambridge, Massachusetts 02138*
- ²³*Division of High Energy Physics, Department of Physics,
University of Helsinki and Helsinki Institute of Physics, FIN-00014, Helsinki, Finland*
- ²⁴*University of Illinois, Urbana, Illinois 61801*
- ²⁵*The Johns Hopkins University, Baltimore, Maryland 21218*
- ²⁶*Institut für Experimentelle Kernphysik,
Universität Karlsruhe, 76128 Karlsruhe, Germany*
- ²⁷*Center for High Energy Physics: Kyungpook National University,
Daegu 702-701, Korea; Seoul National University, Seoul 151-742,
Korea; Sungkyunkwan University, Swon 440-746,*

- Korea; Korea Institute of Science and Technology Information, Daejeon, 305-806, Korea; Chonnam National University, Gwangju, 500-757, Korea*
- ²⁸*Ernest Orlando Lawrence Berkeley National Laboratory, Berkeley, California 94720*
- ²⁹*University of Liverpool, Liverpool L69 7ZE, United Kingdom*
- ³⁰*University College London, London WC1E 6BT, United Kingdom*
- ³¹*Centro de Investigaciones Energeticas Medioambientales y Tecnologicas, E-28040 Madrid, Spain*
- ³²*Massachusetts Institute of Technology, Cambridge, Massachusetts 02139*
- ³³*Institute of Particle Physics: McGill University, Montréal, Canada H3A 2T8; and University of Toronto, Toronto, Canada M5S 1A7*
- ³⁴*University of Michigan, Ann Arbor, Michigan 48109*
- ³⁵*Michigan State University, East Lansing, Michigan 48824*
- ³⁶*University of New Mexico, Albuquerque, New Mexico 87131*
- ³⁷*Northwestern University, Evanston, Illinois 60208*
- ³⁸*The Ohio State University, Columbus, Ohio 43210*
- ³⁹*Okayama University, Okayama 700-8530, Japan*
- ⁴⁰*Osaka City University, Osaka 588, Japan*
- ⁴¹*University of Oxford, Oxford OX1 3RH, United Kingdom*
- ⁴²*University of Padova, Istituto Nazionale di Fisica Nucleare, Sezione di Padova-Trento, I-35131 Padova, Italy*
- ⁴³*LPNHE, Universite Pierre et Marie Curie/IN2P3-CNRS, UMR7585, Paris, F-75252 France*
- ⁴⁴*University of Pennsylvania, Philadelphia, Pennsylvania 19104*
- ⁴⁵*Istituto Nazionale di Fisica Nucleare Pisa, Universities of Pisa, Siena and Scuola Normale Superiore, I-56127 Pisa, Italy*
- ⁴⁶*University of Pittsburgh, Pittsburgh, Pennsylvania 15260*
- ⁴⁷*Purdue University, West Lafayette, Indiana 47907*
- ⁴⁸*University of Rochester, Rochester, New York 14627*
- ⁴⁹*The Rockefeller University, New York, New York 10021*
- ⁵⁰*Istituto Nazionale di Fisica Nucleare, Sezione di Roma 1, University of Rome "La Sapienza," I-00185 Roma, Italy*
- ⁵¹*Rutgers University, Piscataway, New Jersey 08855*

⁵²*Texas A&M University, College Station, Texas 77843*

⁵³*Istituto Nazionale di Fisica Nucleare, University of Trieste/ Udine, Italy*

⁵⁴*University of Tsukuba, Tsukuba, Ibaraki 305, Japan*

⁵⁵*Tufts University, Medford, Massachusetts 02155*

⁵⁶*Waseda University, Tokyo 169, Japan*

⁵⁷*Wayne State University, Detroit, Michigan 48201*

⁵⁸*University of Wisconsin, Madison, Wisconsin 53706*

⁵⁹*Yale University, New Haven, Connecticut 06520*

(Dated: October 29, 2018)

Abstract

We report on the results of a search for standard model Higgs bosons produced in association with W bosons from $p\bar{p}$ collisions at $\sqrt{s} = 1.96$ TeV. The search uses a data sample corresponding to approximately 1 fb^{-1} of integrated luminosity. Events consistent with the $W \rightarrow \ell\nu$ and $H \rightarrow b\bar{b}$ signature are selected by triggering on a high- p_T electron or muon candidate and tagging one or two of the jet candidates as having originated from b quarks. A neural network filter rejects a fraction of tagged charm and light flavor jets, increasing the b -jet purity in the sample and thereby reducing the background to Higgs boson production. We observe no excess $\ell\nu b\bar{b}$ production beyond the background expectation, and we set 95% confidence level upper limits on the production cross section times branching fraction $\sigma(p\bar{p} \rightarrow WH) \cdot Br(H \rightarrow b\bar{b})$ ranging from 3.9 to 1.3 pb, for specific Higgs boson mass hypotheses in the range 110 to 150 GeV/ c^2 , respectively.

PACS numbers: 13.85.Rm, 14.80.Bn

The standard model of elementary particle physics (SM) provides for electroweak gauge symmetry breaking via the Higgs mechanism [1], and the model predicts a single physical remnant of the added Higgs field. This remnant, the Higgs boson H , has yet to be observed experimentally. Results from direct searches at the LEP collider exclude mass values less than $114.4 \text{ GeV}/c^2$ at a 95% confidence level [2], and global fits to precision electroweak data exclude masses greater than $144 \text{ GeV}/c^2$ at 95% confidence level [3]. (Some models beyond the SM predict Higgs bosons whose masses are not constrained by these limits.) For Higgs boson masses just above the range excluded by LEP, the decay to bottom quarks $b\bar{b}$ dominates. Even though gluon fusion $gg \rightarrow H \rightarrow b\bar{b}$ has the largest cross section among Higgs production processes in $p\bar{p}$ collisions [4]), the $b\bar{b}$ data sample is dominated by non-resonant multi-jet background. Consequently, we search for WH production, requiring a leptonic W boson decay to suppress the background. In this Letter we report results of a search for low-mass SM Higgs bosons produced in association with W bosons and decaying to $b\bar{b}$ pairs. The resulting $\ell\nu b\bar{b}$ final state is identified by selecting events with exactly one high-energy electron or muon candidate, large missing transverse energy, and one or two jet candidates having a secondary vertex characteristic of heavy quark decay.

Recent searches at CDF and D0 [5, 6] were limited not only by smaller data samples, but also by contamination from jets associated with charm or light quarks which are falsely tagged as b jets. The search described in this Letter employs for the first time a neural network filter to reject such events, thereby improving the purity of the selected event sample. The data sample of $p\bar{p}$ collisions at $\sqrt{s} = 1.96 \text{ TeV}$ used here corresponds to $0.955 \pm 0.057 \text{ fb}^{-1}$ of integrated luminosity, nearly three times the sample used in previous searches.

The CDF II detector is a general-purpose detector located at the Tevatron $p\bar{p}$ collider at Fermilab [7, 8]. It consists of a cylindrical magnetic spectrometer surrounded by sampling calorimeters used to measure energies of electromagnetic showers and jets. Charged particle tracking is performed with microstrip silicon detectors surrounded by a large cylindrical multilayer drift chamber, both immersed in a solenoidal magnetic field. Jets are identified as a collection of hadronic and electromagnetic calorimeter towers, which are clustered using an iterative cone algorithm with a cone of $\Delta R = \sqrt{(\Delta\phi)^2 + (\Delta\eta)^2} = 0.4$ units in the azimuth-pseudorapidity space [9, 10]. Planar drift chambers used for muon detection surround the calorimeters at least five interaction lengths from the interaction region.

Events are collected using high- p_T electron or muon triggers with a three-level selection filter. The first- and second-level criteria ensure that purely electromagnetic calorimeter clusters exist or that track stubs in the muon chambers align with drift chamber tracks having transverse momentum at least 8 GeV/ c . The third-level trigger ensures that a fully-reconstructed track with p_T at least 18 GeV/ c points to the electromagnetic cluster or muon stub.

Events compatible with the $\ell\nu b\bar{b}$ final state are selected by requiring exactly one electron or muon candidate and missing transverse energy $\cancel{E}_T > 20$ GeV, after jets are corrected for detector imperfections and non-linear calorimeter response [9]. The electron or muon must be within the central part of the detector, in the pseudorapidity regions $|\eta| < 1.1$ or $|\eta| < 1.0$, respectively, and must have transverse energy greater than 20 GeV. The lepton must be isolated from the rest of the event by a cone of radius $\Delta R = 0.4$ containing no more than 10% of the lepton energy (excluding the lepton itself). It must also be no more than 5 cm in z away from the primary event vertex, which is defined by fitting a subset of charged particle tracks in the event to a single vertex. To suppress background from Z boson and diboson production, we reject events with more than one isolated lepton, as well as events in which the lepton and another high-energy track of opposite sign form an invariant mass between 76 and 106 GeV/ c^2 . The requirements for the lepton transverse energy and missing transverse energy reject multi-jet background while maintaining efficiency for the WH signal. Jets used in the analysis must fall within the acceptance of the silicon detector ($|\eta| < 2.0$) for reliable b -tagging, and they must have transverse energy greater than 15 GeV. Even though the $W + 2$ jet final state is the target sample for this search, other samples with $W+1$ or $W+3$, 4 jets are useful for cross-checks of the background estimates with similar topologies.

A B hadron, with relatively long lifetime and large mass, can decay to charged particles whose tracks have large impact parameter, the distance of closest approach to the interaction point in the transverse plane. Such tracks are fit to a secondary vertex, and the decay length of the B hadron is defined as the distance between this vertex and the primary vertex. Specifically, we apply the SECVTX secondary vertex finding algorithm [11] to each jet in the event, using tracks within the $\Delta R = 0.4$ cone centered on the jet axis. Three tracks with impact parameter significances greater than 2.0 are fit to a decay vertex. If this first pass fails, a second pass is attempted with two tracks having impact parameter

significances greater than 3.0. To limit the number of secondary vertices stemming from material interactions, we reject vertices at radii greater than 2.5 cm, as well as any vertices reconstructed within the material of the beampipe and the innermost silicon layer ($1.2 \text{ cm} < r < 1.5 \text{ cm}$). Jets are b -tagged if the magnitude of the significance of the transverse decay length is greater than 7.5. Jets with a negative decay length have a reconstructed flight direction opposite the jet direction. This can happen when tracks coming from the primary vertex have significantly mismeasured impact parameters.

In addition to the secondary vertex finding algorithm, a neural network (NN) filter has been trained with the JETNET program [12] to reject tagged jets originating from charm or light (u, d, s) quarks. When a b quark hadronizes, particles originating at the B hadron vertex tend to carry a large fraction of the jet energy. They also tend to have a higher vertex mass – the invariant mass of all tracks in the secondary vertex – and longer decay lengths than in jets from light quarks. The NN filter uses these jet characteristics to discriminate between b jets and c or light flavor jets. It is composed of two networks in series, one to separate b jets from light quark jets, and the second to separate b jets from c jets. Both networks have the same set of 16 inputs: the number of tracks in the secondary vertex, the χ^2 value of the vertex fit, the transverse decay length and its significance, the vertex mass calculated by assuming the charged pion mass for all particles, the proper time assuming the vertex mass, the fraction of the jet p_T carried by tracks in the vertex, the vertex pass number, the number of tracks with significant impact parameter, the reconstructed mass of the SECVTX pass 1 and pass 2 tracks, the numbers of pass 1 and pass 2 tracks, the fraction of the jet p_T carried by the pass 1 and pass 2 tracks, and finally the probability of a selected ensemble of tracks to have originated at the primary vertex [13]. The selection cuts on the NN output are chosen to give 90% efficiency for true b jets identified with the secondary vertexing algorithm. The corresponding rejection factors are $65 \pm 5\%$ for light flavor jets and $50 \pm 5\%$ for charm jets, as measured using simulated events and verified with multijet data.

Our search criteria select events with exactly one high-energy charged lepton, missing transverse energy, and two jets. The search sensitivity is maximized by defining two distinct subsamples based on the following b -tagging requirements: single-tagged events with exactly one b -tagged jet which passes the NN filter, and double-tagged events with two b -tagged jets. Because events with charm and light-flavor jets are unlikely to be double-tagged, the

extra NN filter is not applied to double-tagged events. The selected event sample includes contributions from other SM processes. The largest background rates are due to W +jets production, $t\bar{t}$ production, and non- W multijet production, with small contributions from electroweak boson production WW or WZ .

The dominant background contribution comes from W +jets production, either with jets from b or c quarks or with jets mistagged by the b -tagging algorithm. The effect of true W +heavy-flavor production is estimated from a combination of data and simulation. We use the ALPGEN Monte Carlo program [14] to calculate the rate of $Wb\bar{b}$, $Wc\bar{c}$, and Wc production relative to inclusive W +jets production. Then this relative rate is applied to the observed W +jets sample, after non- W and $t\bar{t}$ contributions have been subtracted. Finally, we apply a b -tagging efficiency and NN filter rate derived using the ALPGEN event samples.

Events from $t\bar{t}$ production followed by leptonic W decay typically have two b jets from t decay, significant missing transverse energy, and one or two high-energy leptons with two or zero additional jets, depending on whether one or both W bosons from the top quarks decay leptonically. Our selected sample includes contributions from pairs of top quarks which both decay leptonically, but for which the second lepton is not reconstructed. It also includes contributions from pairs of top quarks with one leptonic decay which are selected as two-jet events because two out of four jets do not satisfy the selection criteria. The contribution from $t\bar{t}$ production to the $\ell\nu b\bar{b}$ final state is estimated using simulated PYTHIA events [15]. It is normalized to the NLO cross section $6.7_{-0.9}^{+0.7}$ pb calculated for $m_t = 175$ GeV/ c^2 [16]. The small contribution from production of single top quarks is estimated using MADEVENT [17] and PYTHIA normalized to the NLO cross section [18].

Multijet events may have high-energy identified leptons or missing transverse energies, both mimicking the signature of W decay. These may be from semileptonic heavy flavor decay or from false reconstructions. The identified leptons from such events are rarely isolated in energy, as required by our event selection, and seldom yield large missing transverse energy. We therefore calculate the number of non- W events in our selected sample by extrapolating from sideband regions (defined in the space of lepton energy isolation and missing transverse energy) into the signal region [8].

Contributions from events with falsely tagged light-flavor jets are estimated by measuring a false tag (or mistag) rate in generic jet data. To first order the negative tag rate is a good approximation of the mistag rate because light-flavor jets, whose tracks are prompt, have

Gaussian reconstructed decay length distributions symmetric about zero [11]. The mistag rate is further modified by the NN filter efficiency. The resulting overall mistag rate is applied to the W +jets sample to yield the number of mistagged events present in the sample.

Small contributions from electroweak backgrounds (WW , ZZ , WZ , and $Z \rightarrow \tau\tau$) are estimated using the most recent theoretical cross section calculations [19], with acceptances calculated using fully simulated events from the PYTHIA Monte Carlo program.

The dominant uncertainty in the W + heavy flavor background is the calibration factor for simulation derived from multijet data [8]. Different simulation inputs give different factors, and we find a 35% relative error on the background from heavy flavor. The background from false tags has major uncertainties on the rate correction due to particle interactions in detector material and on the NN rejection factor. Both are 15% relative errors. Cross-checks of sideband data yield a 17% relative uncertainty on the non- W multijet estimate. The electroweak background estimates for diboson and single top are subject to uncertainties in the b -tagging efficiency and the cross section predictions.

We use the large b -tagged sample of W +1 jet events to derive a data-based scaling factor of 1.2 ± 0.2 , which corrects a residual mismatch between the heavy flavor fraction correction factor in multijet data and the W +jets sample. This single factor is applied to the W +heavy flavor background calibration for all jet multiplicities, and it improves the agreement for the sideband multiplicities of W +1, 3, 4 jets. A summary of the estimated background contributions to the lepton + jets sample is shown in Table I, along with the results from the data sample.

The signal process in which a Higgs boson decays to $b\bar{b}$ is expected to show a resonant peak in the dijet mass spectrum. Figures 1 and 2 show the dijet mass spectra in the single- and double-tagged 2-jet samples for the estimated background as well as for the observed events. A $115 \text{ GeV}/c^2$ Higgs boson signal at ten times the SM rate is shown for comparison. There is no significant excess observed in the dijet mass spectrum. The largest discrepancy, for masses near $100 \text{ GeV}/c^2$, is less than one standard deviation defined by the uncertainty on the background estimate.

The acceptance for $WH \rightarrow \ell\nu b\bar{b}$, including leptonic τ decays, is calculated from samples generated with the PYTHIA Monte Carlo program using Higgs boson mass values between 110 and $150 \text{ GeV}/c^2$. Additional efficiency factors include the trigger and identification efficiencies measured separately for the lepton types, and a b -tagging efficiency data-to-

Selection	single NN tag				double tag		
	1 jet	2 jets	3 jets	≥ 4 jets	2 jets	3 jets	≥ 4 jets
Mistag	139.7 ± 27.3	53.9 ± 10.7	15.7 ± 3.1	4.2 ± 0.8	3.5 ± 0.5	2.0 ± 0.3	1.2 ± 0.2
$Wb\bar{b}$	306.9 ± 106.9	144.7 ± 49.4	29.9 ± 9.7	6.4 ± 2.5	20.3 ± 7.0	5.7 ± 1.8	1.0 ± 0.4
$Wc\bar{c}$	63.1 ± 22.0	43.0 ± 14.7	8.7 ± 2.8	1.9 ± 0.8	3.3 ± 1.1	0.4 ± 0.1	0.1 ± 0.04
Wc	185.7 ± 47.2	34.4 ± 9.0	3.4 ± 0.9	0.6 ± 0.2	0.0 ± 0.0	0.0 ± 0.0	0.0 ± 0.0
$t\bar{t}(6.7\text{pb})$	6.9 ± 1.2	42.0 ± 6.6	84.9 ± 12.8	98.6 ± 14.3	10.4 ± 2.3	29.5 ± 6.4	45.5 ± 9.9
Single Top	16.7 ± 1.8	23.5 ± 2.4	4.8 ± 0.5	0.8 ± 0.1	4.2 ± 0.7	1.4 ± 0.2	0.3 ± 0.1
Diboson/ $Z^0 \rightarrow \tau\tau$	11.7 ± 2.2	14.2 ± 2.3	3.9 ± 0.9	1.0 ± 0.3	1.2 ± 0.3	0.3 ± 0.1	0.1 ± 0.1
non- W QCD	84.2 ± 14.1	38.9 ± 6.7	12.1 ± 2.3	5.5 ± 1.2	1.4 ± 0.3	0.9 ± 0.2	0.3 ± 0.1
Total Background	814.9 ± 140.7	394.4 ± 66.6	163.4 ± 18.7	118.9 ± 14.9	44.2 ± 8.5	40.1 ± 6.8	48.6 ± 10.0
Observed Events	856	421	177	139	39	44	65

TABLE I: Background estimate for events with exactly one NN b -tag or double tag as a function of jet multiplicity.

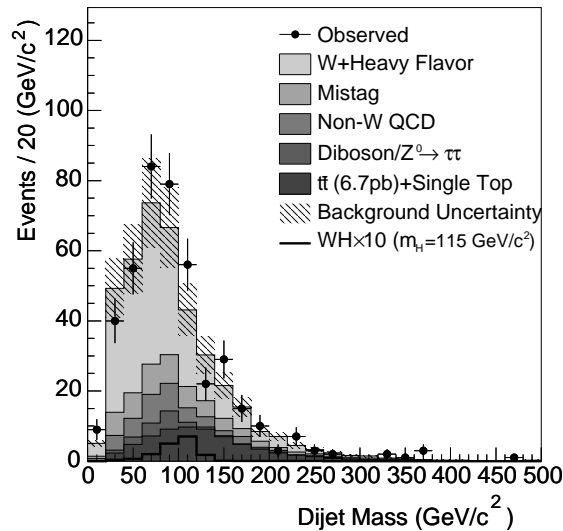


FIG. 1: Reconstructed dijet mass distributions for $W+2$ -jet events with a single b -tag passing the NN filter. The histogram binning is the same used in the binned likelihood calculation.

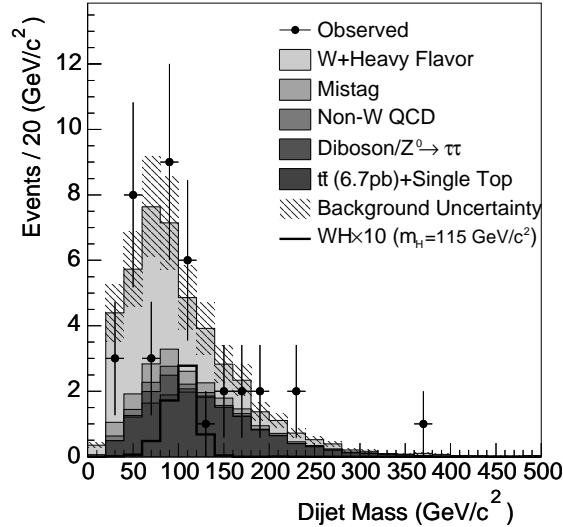


FIG. 2: Reconstructed dijet mass distributions for $W+2$ -jet events with two b -tagged jets. The histogram binning is the same used in the binned likelihood calculation.

simulation scale factor. The acceptances for the single NN tag and double tag selections are $1.3 \pm 0.1\%$ and $0.4 \pm 0.1\%$, including the W branching ratio to lepton pairs, for a mass hypothesis of $115 \text{ GeV}/c^2$. The dominant systematic uncertainty on the acceptance is the b -tagging scale factor uncertainty, which is a 5.3% relative error for the single-tagged selection and a 16% relative error for the double-tagged selection. Variations in the final state radiation model introduce relative uncertainties of 3.2% and 8.6% into the NN single-tagged acceptance and double-tagged acceptance, respectively. Additional sources of systematic error include the jet energy scale, the lepton identification efficiency, and the initial state radiation model [11, 20].

Limits on the number of Higgs boson events, interpreted as the production rate times the branching fraction, are derived using a binned likelihood technique assuming Poisson statistics. The sample is divided into bins of reconstructed dijet mass because the Higgs boson production signal is expected to show a mass resonance. By counting the number of events in each reconstructed mass bin, we discriminate more effectively between the peaked signal and the predicted background shape. Likelihoods are calculated separately for the single-tagged and double-tagged selections. The best exclusion comes from a combination of the single-tagged selection with the NN filter applied and the double-tagged selection.

To calculate the production limits, a Bayesian interval is constructed from the cumulative likelihood distributions and a prior probability density function uniform in the number of Higgs boson signal events s . The 95% confidence level upper limit is defined to be the value s_{up} for which $\int_0^{s_{\text{up}}} L(s) ds / \int_0^{\infty} L(s) ds = 0.95$. The number of signal events is then converted to a Higgs boson production cross section times branching fraction $\sigma(p\bar{p} \rightarrow WH) \cdot Br(H \rightarrow b\bar{b})$.

The observed 95% confidence level upper limits on the cross section times branching fraction range from 3.9 to 1.3 pb, for Higgs boson mass hypotheses from 110 to 150 GeV/c^2 , respectively. Figure 3 summarizes the observed limits as well as the expected limits as a function of the Higgs boson mass hypothesis. A set of background-only pseudoexperiments is generated for each mass; the median limit value in this set defines the expected limit in the absence of signal, and the spread of the pseudoexperiments defines the 1σ band. The observed limit in the low mass region is roughly 2 standard deviations higher than the expected limit.

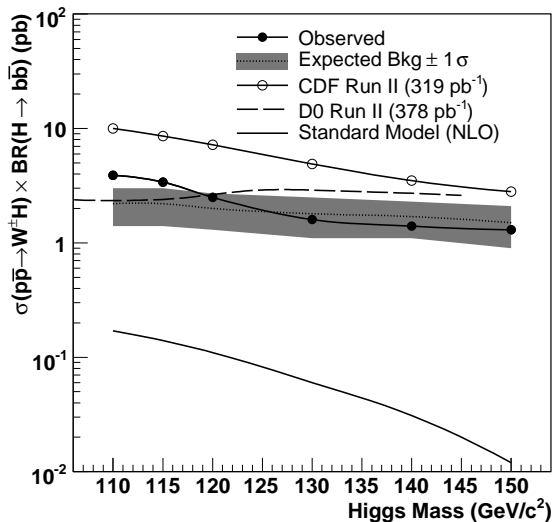


FIG. 3: 95% confidence level upper limit on Higgs boson production cross section times branching fraction as a function of Higgs boson mass hypothesis. The expected limits from background-only pseudoexperiments are shown in addition to the observed results from this search and previous CDF and D0 searches.

In this Higgs boson search, we have employed a novel neural network b -tagging filter on a dataset nearly three times the size of previous searches. The resulting exclusion improves

significantly the limits on the allowed production rate for Higgs bosons in $p\bar{p}$ collisions. Even though the largest improvement by far comes from the larger dataset, separating the single- and double-tag samples results in a 20% improvement beyond the previous analysis, and rejecting charm and light-flavor jets with the NN gains another 5% in sensitivity.

We thank the Fermilab staff and the technical staffs of the participating institutions for their vital contributions. This work was supported by the U.S. Department of Energy and National Science Foundation; the Italian Istituto Nazionale di Fisica Nucleare; the Ministry of Education, Culture, Sports, Science and Technology of Japan; the Natural Sciences and Engineering Research Council of Canada; the National Science Council of the Republic of China; the Swiss National Science Foundation; the A.P. Sloan Foundation; the Bundesministerium für Bildung und Forschung, Germany; the Korean Science and Engineering Foundation and the Korean Research Foundation; the Science and Technology Facilities Council and the Royal Society, UK; the Institut National de Physique Nucleaire et Physique des Particules/CNRS; the Russian Foundation for Basic Research; the Comisión Interministerial de Ciencia y Tecnología, Spain; the European Community's Human Potential Programme; the Slovak R&D Agency; and the Academy of Finland.

-
- [1] P. W. Higgs, Phys. Rev. Lett. **13**, 508 (1964).
 - [2] R. Barate *et al.* (ALEPH, DELPHI, L3, and OPAL collaborations and the LEP Working Group for Higgs boson searches), Phys. Lett. **B565**, 61 (2003), arXiv:hep-ex/0306033.
 - [3] J. Alcaraz *et al.* (ALEPH, DELPHI, L3, and OPAL collaborations and the LEP Electroweak Working Group), Tech. Rep. CERN-PH-EP-2006-042 (2006), arXiv:hep-ex/0612034.
 - [4] T. Han and S. Willenbrock, Phys. Lett. **B273**, 167 (1991).
 - [5] A. Abulencia *et al.* (CDF collaboration), Phys. Rev. Lett. **96**, 081803 (2006), arXiv:hep-ex/0512051.
 - [6] P. M. Jonsson (CDF and DØ collaborations), in *Proceedings of the 41st Rencontres de Moriond: QCD and Hadronic Interactions* (2006), arXiv:hep-ex/0605088.
 - [7] D. Acosta *et al.* (CDF collaboration), Phys. Rev. D **72**, 052003 (2005), arXiv:hep-ex/0504053.
 - [8] D. Acosta *et al.* (CDF collaboration), Phys. Rev. D **71**, 052003 (2005), arXiv:hep-ex/0410041.
 - [9] The CDF reference frame uses cylindrical coordinates, where z is the direction of the proton

beam, and θ and ϕ are the polar and azimuthal angles with respect to the proton beam. The pseudorapidity is defined as $\eta = -\ln \tan \theta/2$, the transverse energy $E_T = E \sin \theta$, and the transverse momentum $p_T = p \sin \theta$. The \cancel{E}_T magnitude is the vector sum of all calorimeter deposits, projected into the transverse plane. The \cancel{E}_T vector is corrected for the energy deposition of the high-energy muons as well as for the jet energy corrections.

- [10] F. Abe *et al.* (CDF collaboration), Phys. Rev. D **45**, 1448 (1992).
- [11] A. Abulencia *et al.* (CDF collaboration), Phys. Rev. Lett. **97**, 082004 (2006), arXiv:hep-ex/0606017.
- [12] C. Peterson, T. Rognvaldsson, and L. Lönnblad, Comput. Phys. Commun. **81**, 185 (1994).
- [13] A. Abulencia *et al.* (CDF collaboration), Phys. Rev. D **74**, 072006 (2006), arXiv:hep-ex/0607035.
- [14] M. L. Mangano, M. Moretti, F. Piccinini, R. Pittau, and A. D. Polosa, J. High Energy Phys. **07**, 001 (2003), arXiv:hep-ph/0206293.
- [15] T. Sjöstrand *et al.*, Comput. Phys. Commun. **135**, 238 (2001), arXiv:hep-ph/0010017.
- [16] M. Cacciari, S. Frixione, G. Ridolfi, M. L. Mangano, and P. Nason, J. High Energy Phys. **04**, 068 (2004), arXiv:hep-ph/0303085.
- [17] F. Maltoni and T. Stelzer, J. High Energy Phys. **02**, 027 (2003), arXiv:hep-ph/0208156.
- [18] B. W. Harris, E. Laenen, L. Phaf, Z. Sullivan, and S. Weinzierl, Phys. Rev. D **66**, 054024 (2002), arXiv:hep-ph/0207055.
- [19] J. M. Campbell and R. K. Ellis, Phys. Rev. D **60**, 113006 (1999), arXiv:hep-ph/9905386.
- [20] A. Bhatti *et al.* (CDF collaboration), Nucl. Instrum. Methods A **566**, 375 (2006), arXiv:hep-ex/0510047.